Available online at www.sciencedirect.com
ScienceDirect
Journal of Power Sources 175 (2008) 680–685
JOURNAL OF POWER SOURCES
www.elsevier.com/locate/jpowsour

Short communication

Potentiostatically deposited nanostructured Co_xNi_{1-x} layered double hydroxides as electrode materials for redox-supercapacitors

Vinay Gupta [a,b,*], Shubhra Gupta [a], Norio Miura [a,*]

[a] *Art, Science and Technology Center for Cooperative Research, Kyushu University, Kasuga-shi, Fukuoka 816-8580, Japan*
[b] *Japan Science and Technology Agency, Kawaguchi-shi, Saitama 332-0012, Japan*

Received 29 August 2007; received in revised form 4 September 2007; accepted 5 September 2007
Available online 11 September 2007

Abstract

Cobalt–nickel layered double hydroxides (Co_xNi_{1-x} LDHs) were deposited onto stainless steel electrodes by the potentiostatic deposition method at −1.0 V vs. Ag/AgCl using various molar ratios of $Co(NO_3)_2$ and $Ni(NO_3)_2$ in distilled water. Their structure and surface morphology were studied by using X-ray diffraction analysis, energy dispersive X-ray spectroscopy and scanning electron microscopy. A network of Co_xNi_{1-x} LDH nanosheets was obtained. The nature of the cyclic voltammetry and charge–discharge curves suggested that the Co_xNi_{1-x} LDHs exist in the form of solid solutions. The capacitive characteristics of the Co_xNi_{1-x} LDHs in 1 M KOH electrolyte showed that $Co_{0.72}Ni_{0.28}$ LDHs had the highest specific capacitance value, 2104 F g^{-1}, which is also the highest yet reported value for oxide materials in general.

Keywords: Co_xNi_{1-x} LDHs; Potentiostatic deposition; Specific capacitance; Supercapacitor

1. Introduction

Supercapacitors combine the advantages of both high power density and high energy density. Supercapacitors are important for use in hybrid electrical vehicles to provide peak power during acceleration in combination with batteries [1–3]. They are a key to the future development of mobile technology and microelectromechanical systems. Supercapacitors can be charged by two different mechanisms: (1) electrical double-layer charging and (2) redox-type charge transfer. In double-layer charging, the electrical charge is stored at the interface between the electrode and electrolyte; thus, such devices are termed electrical double layer capacitors (EDLC). In contrast, redox-type charge transfer arises from reversible Faradaic reactions taking place at the interface between the electrode and electrolyte in an appropriate potential range; these devices are termed pseudocapacitors or redox capacitors.

Redox capacitors can have much higher specific capacitance than EDLCs [4]. The most notable among them are noble metals. In particular, RuO_2 can have a specific capacitance as high as 760 F g^{-1} [5,6], but it cannot be used in practical applications due to high cost. Therefore, other metal oxides, such as nickel oxide [7], cobalt oxide [8] and manganese oxide [9], have been explored for their capacitive characteristics due to the fact that they exhibit pseudocapacitive behavior similar to that of RuO_2. However, such metal oxides have exhibited lower specific capacitance as compared to RuO_2.

Recent development of metal hydroxides with high specific capacitances has regenerated great interest in such materials [10–15]. Metal hydroxides are often layered materials with large interlayer spacing [16,17]. They can have very high theoretical specific capacitances. A recent synthesis of nanoporous nickel hydroxide films by means of a hexagonal lyotropic liquid crystalline phase of Brij 56 (poly(oxyethylene) cetyl ether) showed a maximum specific capacitance of 578 F g^{-1} [10]. In the case of Co–Al layered double hydroxides, a maximum specific capacitance of 684 F g^{-1} was observed [11], whereas in the case of $Ni(OH)_2$/activated carbon composite, a specific capacitance value of 530 F g^{-1} was reported [12]. $Co(OH)_2$/Y-zeolite composites showed a total specific capacitance of 1492 F g^{-1}

* Corresponding author at: Art, Science and Technology Center for Cooperative Research, Kyushu University, Kasuga-shi, Fukuoka 816-8580, Japan. Tel.: +81 92 583 7886; fax: +81 92 583 8976.
E-mail address: vinay@astec.kyushu-u.ac.jp (V. Gupta).

0378-7753/$ – see front matter © 2007 Elsevier B.V. All rights reserved.
doi:10.1016/j.jpowsour.2007.09.004

Table 1
EDX analysis of Co, Ni and O in Co_xNi_{1-x} LDHs, potentiostatically deposited in various given molar concentrations of $Co(NO_3)_2{\cdot}6H_2O$ and $Ni(NO_3)_2{\cdot}6H_2O$

Electrolyte solution Co:Ni	Co (atomic%)	Ni (atomic%)	O (atomic%)	$[Co(OH)_2]_x[Ni(OH)_2]_{1-x}$ (x)
0.25 M:0.75 M	13.3	18.9	67.8	0.41
0.50 M:0.50 M	20.6	11.4	68.0	0.62
0.60 M:0.40 M	23.0	9.1	67.9	0.72
0.75 M:0.25 M	26.0	6.0	68.0	0.81

[13]. In the case of $Co(OH)_2$–$Ni(OH)_2$/Y-zeolite composites, a specific capacitance of 479 F g^{-1} was obtained [14]. The previously reported metal hydroxides were mainly prepared by the precipitation process, which has a disadvantage due to the agglomeration of particles during preparation, large particle size and requirement of a binder. In this work, we have prepared Co_xNi_{1-x} LDHs by the potentiostatic deposition method and have obtained very high specific capacitances. This work opens up further possibilities for achieving nanomaterial composites with high specific capacitances.

2. Experimental

Analytical grade chemicals ($Co(NO_3)_2{\cdot}6H_2O$, $Ni(NO_3)_2{\cdot}6H_2O$ and 1 M KOH) and research grade stainless-steel (SS, grade 304, 0.2 mm thick) were used for the Co_xNi_{1-x} LDH preparations. In the initial measurements, we used SS electrodes of several sizes from 1 cm × 1 cm to 6 cm × 8 cm. It was found that the supercapacitive characteristics are almost independent of the electrode size. The deposition was homogenous in all cases. However, in this work, the area of the SS favored for deposition was 6 cm × 8 cm from the viewpoint of practical applications. The SS was polished with emery paper to a rough finish, washed free of abrasive particles and then air-dried. An electrochemical cell was assembled in a three-electrode configuration in which the counter electrode was platinum (Pt), the reference electrode was Ag/AgCl (saturated KCl solution) and the working electrode was SS. The molar concentrations of the $Co(NO_3)_2{\cdot}6H_2O$:$Ni(NO_3)_2{\cdot}6H_2O$ aqueous solutions were 0.25:0.75, 0.50:0.50, 0.60:0.40 and 0.75:0.25; these were used for the potentiostatic deposition of Co_xNi_{1-x} LDHs onto SS. The potentiostatic deposition was carried out at a potential of −1.0 V vs. Ag/AgCl. The details of the potentiostatic deposition method are given elsewhere [9].

The deposited electrodes were washed in distilled water by using a magnetic paddle in a beaker and then dried in an oven at 50 °C overnight. The weight of the deposit was measured by means of a micro-balance (Sartorius, BP211D) with an accuracy of 0.01 mg. The weights of all deposited Co_xNi_{1-x} LDHs were ∼10 mg. The deposition was controlled by monitoring the Coulombic charge. The elemental analysis was carried out by use of an energy dispersive X-ray (EDX) spectrometer (EDAX, Horiba EX-220SE) coupled to a scanning electron microscope (Hitachi, S3000-N). The microstructure of the electrode materials was evaluated by use of a field emission scanning electron microscope (FE-SEM, JEOL, JSM-6340F). The X-ray diffraction patterns were obtained by use of an X-ray diffractometer (XRD, RIGAKU, R1NT2100) with Cu Kα radiation (λ = 1.5406 Å) operating at 40 kV, 20 mA. The TG/DTA curves were obtained by using an SII TG/DTA analyzer (Model 3200). The particle size distribution measurements were performed using laser scattering particle size analyzer (HORIBA, LB 500X). The particle size distribution was measured in the particle size range of 0.003–1 μm and 1–100 μm range separately using two different apparatus. The surface area analyses were done using Macrosorb automatic surface area analyzer (MOUN-

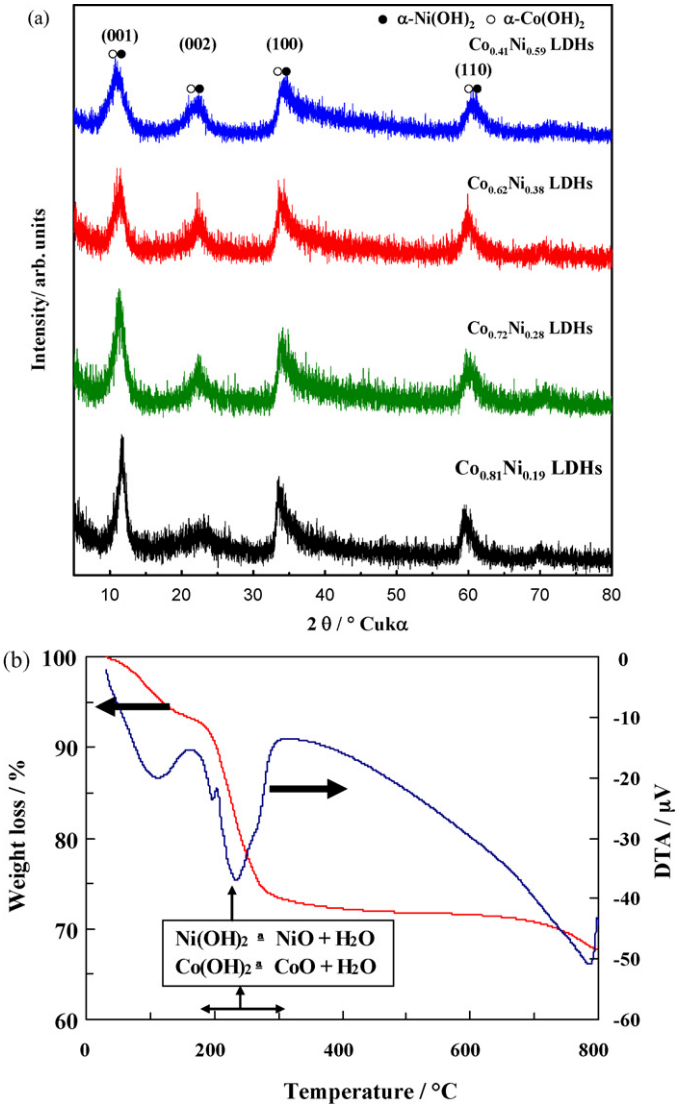

Fig. 1. (a) XRD patterns of the Co_xNi_{1-x} LDHs; (b) TG/DTA curves of the $Co_{0.72}Ni_{0.28}$ LDHs.

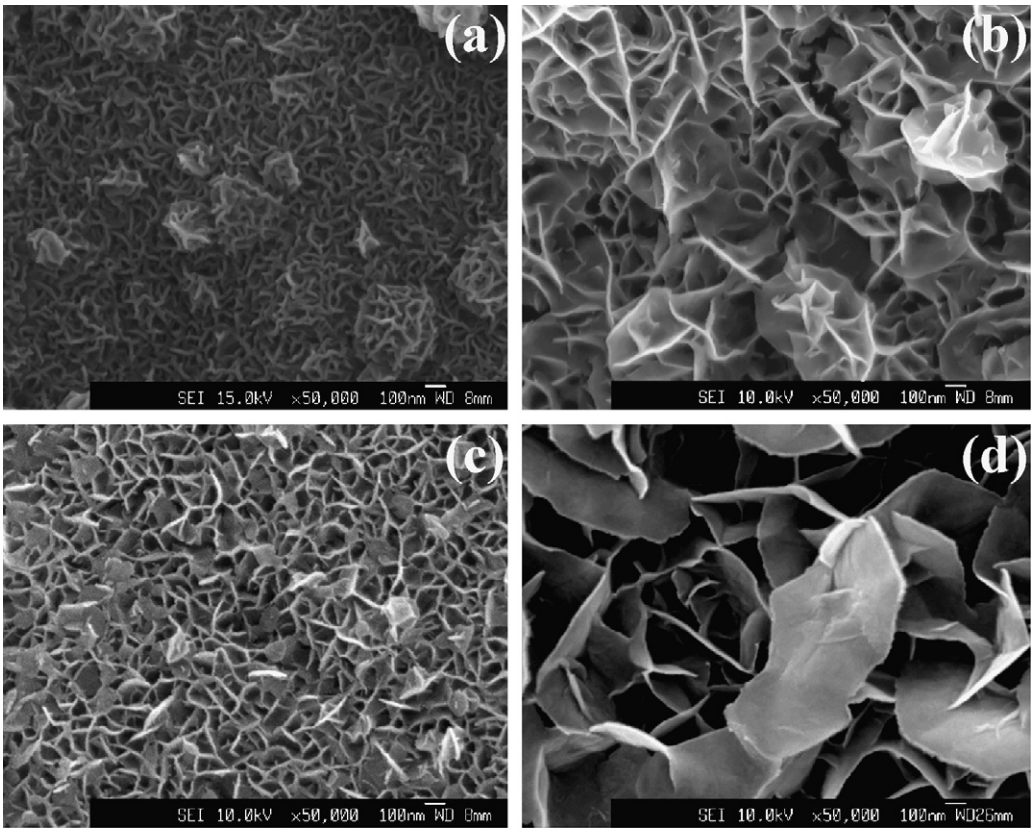

Fig. 2. SEM images of the Co_xNi_{1-x} LDHs with x values of (a) 0.41; (b) 0.62; (c) 0.72; (d) 0.81.

TECH, HM-Model 120). All electrochemical depositions and capacitive measurements were performed by use of a potentiostat (AUTOLAB®, Eco Chemie, PGSTAT 30). The capacitive characterization was performed in 1 M KOH electrolyte.

3. Results and discussion

Table 1 shows the atomic percentages (at%) of the elements Co, Ni and O in Co_xNi_{1-x} LDHs, obtained by means of EDX spectroscopy. The elemental composition indicates that the Co_xNi_{1-x} LDHs are composed of $Co(OH)_2$ and $Ni(OH)_2$, as the amount of oxygen was slightly higher than twice those of Co and Ni combined. The slightly higher content of oxygen (~3 at%) may due to water of hydration as well as absorbed water. From the EDX analysis, the exact formula of the Co_xNi_{1-x} LDHs would be $[Co(OH)_2]_x[Ni(OH)_2]_{1-x}\cdot 0.1H_2O$ with $x = 0.41$, 0.62, 0.72 and 0.81, obtained from the depositions carried out in $Co(NO_3)_2\cdot 6H_2O$:$Ni(NO_3)_2\cdot 6H_2O$ solutions of molar concentrations 0.25:0.75, 0.50:0.50, 0.60:0.40 and 0.75:0.25, respectively.

Fig. 1a shows the XRD patterns of the Co_xNi_{1-x} LDH composites. The patterns in Fig. 1a comprise four broad peaks appearing at 2θ values of 11.4° (7.75 Å), 22.7° (3.81 Å), 34.0° (2.68 Å) and 59.6° (1.55 Å). The XRD diffraction patterns correspond to both α-$Co(OH)_2$ and α-$Ni(OH)_2$. It was difficult to differentiate between the two phases, since they have similar structures, and their diffraction peaks are very close. Fig. 2b shows the TG/DTA curves of the deposited $Co_{0.72}Ni_{0.28}$ LDHs in 100 ml min^{-1} N_2 flow. The TG curve shows an initial weight loss of 8–9% at around 100 °C, which is due to the desorption of physically adsorbed water, and thereafter, the main weight loss of 18–19%, in the temperature range of 180–300 °C, may be due to the decomposition of the $Co_{0.72}Ni_{0.28}$ LDH into the respective oxides, as shown in the inset of Fig. 1b. Since the loss of water of hydration occurs in the similar temperature range, its amount could not be estimated. The TG/DTA curves were similar for all of the deposits.

The SEM images of the deposited Co_xNi_{1-x} LDHs are shown in Fig. 2. For the $Co_{0.41}Ni_{0.59}$ LDH, a dense microstructure was observed (Fig. 2a). The microstructure becomes thin and less dense for the $Co_{0.62}Ni_{0.38}$ LDH (Fig. 2b). The microstructure of the composite changed to nanostructure for the $Co_{0.72}Ni_{0.28}$ LDH (Fig. 2c). For the $Co_{0.81}Ni_{0.19}$ LDH, the sheet size again increased (Fig. 2d). The average thickness of the sheets in Figs. 2b–d was ~10 nm, whereas it was in the range of 20–30 nm in Fig. 2a. Fig. 3a shows a high magnification SEM image of $Co_{0.72}Ni_{0.28}$ LDH whereas the cross-section area of $Co_{0.72}Ni_{0.28}$ LDH deposit is shown in Fig. 3b. The thicknesses were several micrometers for all the deposits. Fig. 3c shows the particle size distribution of $Co_{0.72}Ni_{0.28}$ LDH deposit. The low particle size distribution, centered at 10 nm, is due the thickness of the nanosheets, whereas the distribution, centered at 1 μm, is along the surface direction, which is higher than the observed ~100 nm size (Fig. 2c) due to the aggregation of the nanosheets.

Fig. 4a and b shows the CV curves of the $Co(OH)_2$, $Ni(OH)_2$ and Co_xNi_{1-x} LDH electrodes in 1 M KOH electrolyte at the

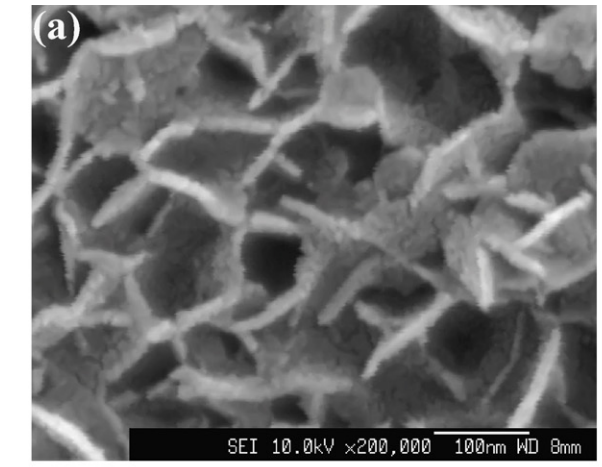

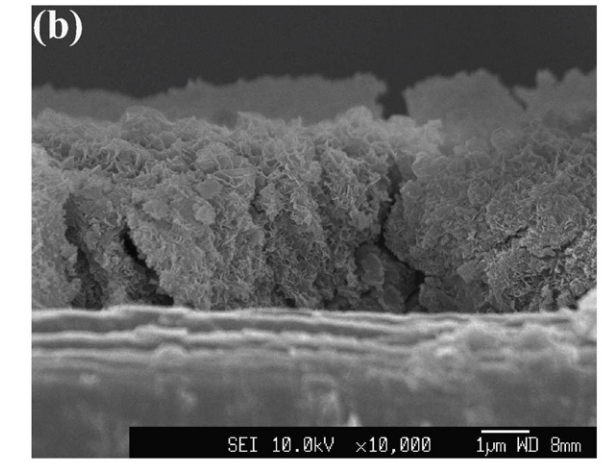

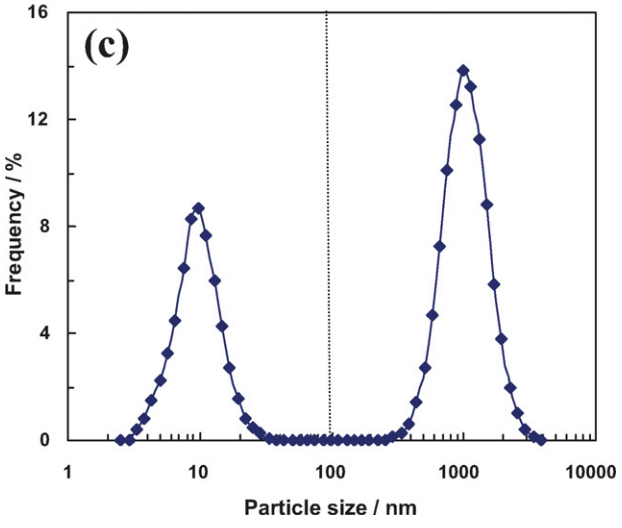

Fig. 3. (a) High magnification SEM image; (b) cross-sectional SEM image; (c) particle size distribution of $Co_{0.72}Ni_{0.28}$ LDHs.

scan rate of 10 mV s^{-1} in the potential range of −1.0 V to +0.6 V. The $Co(OH)_2$, $Ni(OH)_2$ and Co_xNi_{1-x} LDH electrodes showed very strong redox peaks due to the following Faradaic reactions of $Co(OH)_2$ and $Ni(OH)_2$ [14]:

$$Co(OH)_2 + OH^- \Leftrightarrow CoOOH + H_2O + e^- \quad (1)$$

$$CoOOH + OH^- \Leftrightarrow CoO_2 + H_2O + e^- \quad (2)$$

$$Ni(OH)_2 + OH^- \Leftrightarrow NiOOH + H_2O + e^- \quad (3)$$

The CV curves showed shifts in the redox peaks as the compositions of the Co_xNi_{1-x} LDHs were changed, as shown in Fig. 4b. It can be seen that the oxidation and reduction peaks for the $Co_{0.41}Ni_{0.59}$ LDH are at 0.4 V and 0.1 V, respectively, whereas for the $Co_{0.72}Ni_{0.28}$ LDH, the peaks are at 0.1 V and −0.05 V for the oxidation and reduction processes, respectively. The redox current is highest for the $Co_{0.72}Ni_{0.28}$ LDH.

Fig. 4c and d shows the charge–discharge (CD) curves of the $Co(OH)_2$, $Ni(OH)_2$ and Co_xNi_{1-x} LDH electrodes in 1 M KOH electrolyte at 1 A g^{-1} current in the potential range between 0 and 0.4 V. One can observe redox characteristics in the CD curves which are directly related to the redox peaks in the CV curves (Fig. 4a and b). From Fig. 4c, specific capacitance values of 323 F g^{-1} and 860 F g^{-1} were obtained for $Ni(OH)_2$ and $Co(OH)_2$ [18], respectively. Another important aspect of a supercapacitor electrode is its resistance. Fig. 4e and f shows the electrochemical impedance spectra in the form of Nyquist plots for $Co(OH)_2$ and Co_xNi_{1-x} LDHs electrodes at 0.2 V and at 0.4 V in the case of $Ni(OH)_2$, where Z' and Z'' are the real and imaginary parts of the impedance, respectively. The plots obtained are composed of a semi-circle at high frequencies, which is related to Faradaic reactions. The slope close to 45° along the imaginary axis (Z'') at low frequencies is due to a Warburg impedance (a limiting diffusion process), and is not useful for charge storage. From Fig. 4e and f, the observed electrode resistances was close to 0.05 Ω for Co dominated composites and increases as the Ni content in the composite is increased. The highest electrode resistance was observed for $Ni(OH)_2$, which was close to 1 Ω. This shows that all the electrodes in the present study were of a highly conducting nature.

Fig. 5 shows the specific capacitance values as a function of x in the Co_xNi_{1-x} LDHs, obtained from charge–discharge curves. It is noteworthy that a very high specific capacitance, 2104 F g^{-1}, is observed for $Co_{0.72}Ni_{0.28}$ LDH at 1 A g^{-1}. Cao et al. [13] have shown that in the case of $Co(OH)_2$–$Ni(OH)_2$/Y-zeolite composites, the contribution of $Co(OH)_2$–$Ni(OH)_2$ is estimated to be 1710 F g^{-1}. However, the total specific capacitance value was 479 F g^{-1} in their case due to the presence of zeolites. Here we were able to obtain a very high specific capacitance without the use of zeolites. The observation of such a high specific capacitance cannot be explained by N_2 absorption BET surface area analysis, because hydroxide materials lacks micro-pores that can absorb N_2 [19]. In the present case, the amount of N_2 absorption decreases as the Ni content in the LDHs is increased. Surface areas of 35.7 m^2 g^{-1}, 3.9 m^2 g^{-1} and 1.9 m^2 g^{-1} were obtained for $Co_{0.81}Ni_{0.19}$ LDHs, $Co_{0.72}Ni_{0.28}$ LDHs and $Co_{0.62}Ni_{0.38}$ LDHs, respectively whereas no surface area was obtained for $Co_{0.41}Ni_{0.59}$ LDHs because no N_2 absorption took place. However, for $Co_{0.72}Ni_{0.28}$ LDHs, high magnification SEM images showed a very astounding feature in which the LDHs sheets seemed to be composed of aggregated nanometer size particles, instead of flat surface, as shown in Fig. 3a. This porous structure with inter-particles spaces can accommodate electrolyte and increases the electrochemically active sites and therefore can improve utilization of the LDHs. This feature was not observed

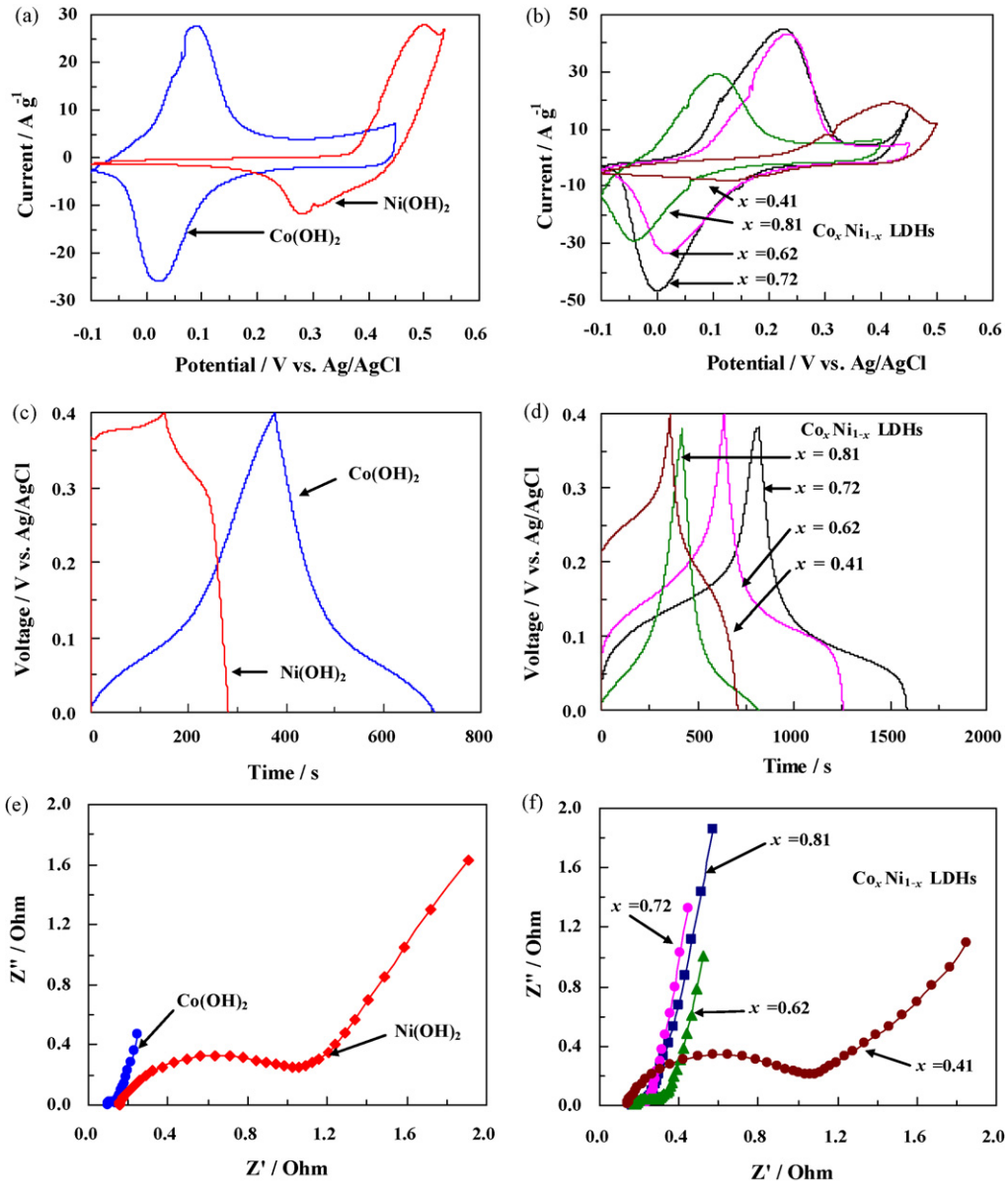

Fig. 4. (a) and (b) Cyclic voltammograms; (c) and (d) charge–discharge curves; (e) and (f) Nyquist plots of $Co(OH)_2$, $Ni(OH)_2$ and Co_xNi_{1-x} LDHs.

for other Co_xNi_{1-x} LDHs. The electrochemical utilization of an electrode can be calculated from the following equation [7].

$$Z = C \cdot \Delta V \cdot \frac{M}{F} \tag{4}$$

where C is the real specific capacitance ($F\,g^{-1}$); ΔV is the potential window (0.4 V in this work), M is an average molecular weight of Co_xNi_{1-x} LDHs (92.8 g mol^{-1}) and F is the Faradic constant. If all the electro-active sites are involved in the faradic reactions, the z value corresponds to 1. The calculation from Eq. (4) gives z values of 0.335, 0.617, 0.809 and 0.414 for Co_xNi_{1-x} LDHs with x values of 0.41, 0.62, 0.72 and 0.81, respectively. Among the LDHs, $Co_{0.72}Ni_{28}$ LDHs possesses the highest z value of 80.9%. In other words, almost 80.9% of the electro-active sites participated in the redox reaction, thus giving the maximum specific capacitance of 2104 $F\,g^{-1}$. The preliminary results on long-term charge–discharge tests suggest the stability characteristics similar to that of reported previously [14].

In conclusion, Co_xNi_{1-x} LDHs with anisotropic morphology were synthesized by the potentiostatic deposition method. Such morphology provided an accessible pathway for the intercalation of OH^- ions into the composite, as the interlayer space of the Co_xNi_{1-x} LDHs is compatible with the size of the hydrated ions (6–7.6 Å). The highest capacitance, 2104 $F\,g^{-1}$, was observed for the $Co_{0.72}Ni_{0.28}$ LDH. The potentiostatic deposition method for the preparation of Co_xNi_{1-x} LDHs is expected to be applied to other systems.

Acknowledgements

The present work was supported by the Japan Science and Technology (JST) Agency through the Core Research for Evo-

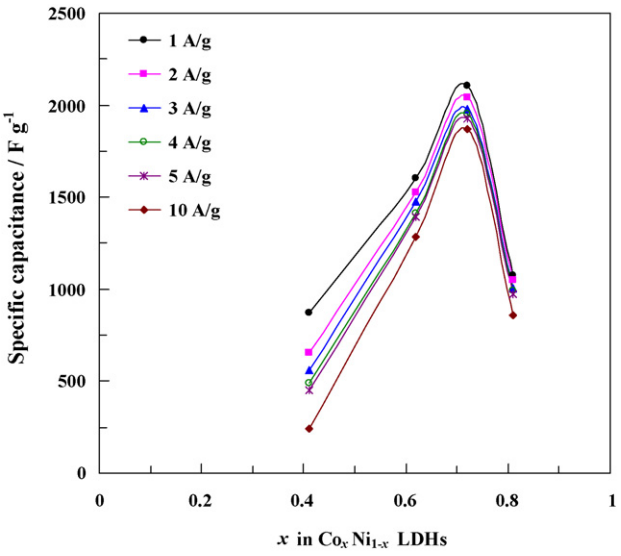

Fig. 5. Specific capacitances of the Co_xNi_{1-x} LDHs as a function of x.

lutionary Science and Technology (CREST) program under the project "Development of advanced nanostructured materials for energy conversion and storage."

References

[1] B.E. Conway, Electrochemical Supercapacitors, Kulwar Academic/Plenum Publishers, New York, 1999, p. 1.
[2] L.T. Lam, R. Louey, J. Power Sources 158 (2006) 1140.
[3] J.R. Miller, Electrochim. Acta 52 (2006) 1703.
[4] T.A. Centeno, F. Stoeckli, in: V. Gupta (Ed.), Recent Advances in Supercapacitors, Transworld Research Network, Kerala, India, 2006, p. 57.
[5] J.H. Jang, K. Machida, Y. Kim, K. Naoi, Electrochem. Acta 52 (2006) 1733.
[6] C.C. Hu, T.W. Tsou, Electrochim. Acta 47 (2002) 3523.
[7] K.W. Nam, K.W. Kim, J. Electrochem. Soc. 149 (2002) A346.
[8] V. Srinivasan, J.W. Weidner, J. Power Sources 108 (2002) 15.
[9] T. Shinomiya, V. Gupta, N. Miura, Electrochem. Acta 51 (2006) 4412.
[10] D.D. Zhao, S.S. Bao, W.J. Zhou, H.L. Li, Electrochem. Commun. 9 (2007) 869.
[11] Y. Wang, W. Yang, S. Zhang, D.G. Evans, X. Duan, J. Electrochem. Soc. 152 (2005) A2130.
[12] J.H. Park, O.O. Park, K.H. Shin, C.S. Jin, J.H. Kim, Electrochem. Solid State Lett. 5 (2002) H7.
[13] L. Cao, F. Xu, Y.Y. Liang, H.L. Li, Adv. Mater. 16 (2004) 1853.
[14] Y.Y. Liang, S.J. Bao, H.L. Li, J. Solid State Electrochem. 11 (2007) 571.
[15] C.C. Hu, C.Y. Cheng, Electrochem. Solid-State Lett. 5 (2002) A43.
[16] R.S. Jayashree, P.V. Kamath, J. Mater. Chem. 9 (1999) 961.
[17] T.N. Ramesh, M. Rajamathi, P.V. Kamath, Solid State Ionics 5 (2003) 751.
[18] V. Gupta, N. Miura, Electrochem. Commun. 9 (2007) 2315.
[19] M. Herrero, P. Benito, F.M. Labajos, V. Rives, J. Solid State Chem. 180 (2007) 873.